J Therm Anal Calorim (2011) 104:963–967
DOI 10.1007/s10973-011-1315-1

Thermal and optical properties of Cu(II)-doped magnesium rubidium sulfate hexahydrate crystals

H. Anandalakshmi · S. Parthiban · V. Parvathi · V. Thanikachalam · S. C. Mojumdar

CTAS2010 Conference Special Chapter
© Akadémiai Kiadó, Budapest, Hungary 2011

Abstract Single crystals of pure and cupric ion (Cu(II))-doped magnesium rubidium sulfate hexahydrate (MRSH) were prepared by slow evaporation of saturated solution technique (SEST) and the influence of dopant Cu(II) on the MRSH crystals has been investigated. Incorporation of Cu(II) into the crystalline matrix was confirmed by energy dispersive spectroscopy (EDS) and electron paramagnetic resonance (EPR) spectroscopy. Thermogravimetric (TG) analysis of the doped sample reveals the faster rate of degradation. EPR spectrum of the MRSH both at room temperature and at 77 K indicates the presence of Cu(II) in the interstitial position. The grown crystals were also characterized by UV–VIS and IR spectroscopy. The surface morphology of the doped sample studied by scanning electron microscopy (SEM) indicates different morphology at various magnifications. The non-linear optical (NLO) property measured using second harmonic generation (SHG) efficiency test reveals that the non-linearity is not facilitated by doping of Cu(II).

Keywords Crystal growth · Tutton's salts · TG · DTA · EPR spectra

H. Anandalakshmi · S. Parthiban
Department of Chemistry, Faculty of Engineering and Technology, Annamalai University, Annamalainagar, Chidambaram, Tamilnadu 608 002, India

V. Parvathi · V. Thanikachalam
Chemistry Wing, DDE, Annamalai University, Annamalainagar, Chidambaram, Tamilnadu 608 002, India

S. C. Mojumdar
University of New Brunswick, Fredericton, NB E3B 5A3, Canada

S. C. Mojumdar (✉)
Department of Chemical and Biochemical Engineering, The University of Western Ontario, London, ON N6A 5B9, Canada
e-mail: scmojumdar@yahoo.com

S. C. Mojumdar
Department of Chemical Technologies and Environment, Faculty of Industrial Technologies, Trencin University of A. Dubcek, Púchov, Slovakia

Introduction

The cupric ion (Cu(II))-doped magnesium rubidium sulfate hexahydrate (MRSH) crystal which comes under the category of Tutton's salts was prepared with a relative ease. Tutton salts have the general formula $M_1''M_2'(XPO_4)_2\cdot 6H_2O$, where M'' is a divalent cation like Co, Cu, Ni, Mg, and M' is a monovalent cation like K, Cs, Rb, and X is S or Se. Tutton's salts were of historical importance because they were obtainable in high purity and served as reliable reagents and spectroscopic standards [1]. Many works have been reported to study the doping effects of paramagnetic ions in Tutton's salts [2–4]. The paramagnetic resonance studies of copper ion doped Tutton's salt has been reported [5]. The Cu^{2+}-doped $Na_2Zn(SO_4)_2\cdot 4H_2O$ shows that in EPR spectra Z axis of the rhombic field falls along Zn–O($H_2O_{(1)}$) direction [6]. In EPR investigation of Cu(II)-doped thallium magnesium sulfate hexahydrate, the Cu^{2+} ions are found to substitute for divalent cations exhibiting two symmetry related equivalent complexes [7]. Silver and Getz showed that the temperature dependence of the EPR spectrum of ~1% Cu^{2+} doped into the potassium zinc(II) Tutton salt could be interpreted satisfactorily [8]. The influence of surface magnetic coupling on the thermal boundary resistance between a magnetic salt and liquid He below 100 mK on $CuK_2(SO_4)_2\cdot 6H_2O$ Tutton's salt has been reported [9]. Crystal growth of large $Rb_2Ni(SO_4)_2{\cdot}6H_2O$ has been studied [10]. The Cu^{2+} doping on glycine lithium sulfate reveals interesting feature [11]. Thermal, microscopic, X-ray, and spectral analyses are very important methods in materials characterization. Therefore, many authors have applied these techniques for various materials characterization [12–21]. Recently, we have studied doping effects of metals on some technologically important crystals [22–24]. In this investigation, the paramagnetic Cu^{2+} ion doping effects on $MgRb_2(SO_4){\cdot}6H_2O$ by using various experimental techniques have been studied and useful conclusions are made.

Experimental

Synthesis and crystal growth

Pure MRSH was prepared by mixing equimolar concentrations (1:1) of $MgSO_4$ (24.6 g) and Rb_2SO_4 (26.7 g). A small amount of (about 1 mol%) of paramagnetic impurity Cu(II) in the form of $CuSO_4$ solution was used for doping. The solution was stirred at 30 °C and slow evaporation method was used for the growth of the crystals from aqueous solution. Pure MRSH crystal is colorless when formed while Cu(II)-doped is light blue in color. Photographs of the crystals grown from pure and Cu(II)-doped MRSH are shown in Fig. 1.

Measurements

The FTIR spectra were recorded for both pure and doped samples on an AVATAR 330 FTIR instrument using the KBr pellet technique in the range 500–4,000 cm^{-1}.

The surface morphology was observed using a JEOL JSM 5610 LV SEM. In the SEM, the image is formed and presented by a very fine electron beam, which is focused on the surface of the specimen. At any given moment, the specimen is bombarded with electrons over a very small area. EDS is a chemical microanalysis technique performed in conjunction with a SEM. The technique utilizes X-rays that are emitted from the sample during bombardment by the electron beam to characterize the elemental composition of the analyzed volume. When the sample is bombarded by the electron beam of the SEM, electrons are ejected from the atoms comprising the sample's surface. A resulting electron vacancy is filled by an electron from a higher shell and an X-ray is emitted to balance the energy difference between the two electrons. The energy of the X-ray is characteristic of the element from which the X-ray was emitted. A spectrum of the energy versus relative counts of the detected X-rays is obtained and evaluated for qualitative and quantitative determinations of the elements present in the sampled volume. This method can detect elements from Na upward in the periodic table.

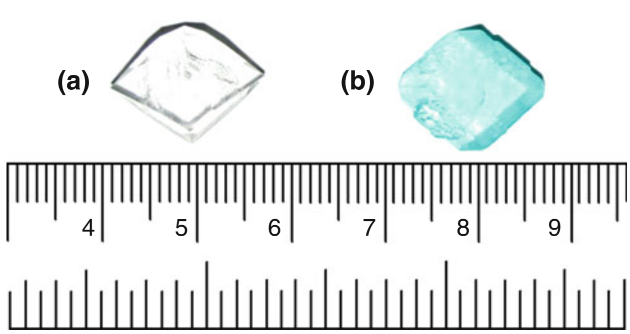

Fig. 1 Photographs of **a** MRSH and **b** Cu(II)-doped MRSH

TG-DTA curves were recorded on a SDT Q600 (TA instruments) thermal analyzer with a heating rate of 10 °C/min at room temperature to 700 °C.

EPR spectra were recorded on a JEOL JES-TE100 ESR spectrometer operating at X-band frequencies, having a 100 kHz field modulation to obtain a first derivative EPR spectrum. DPPH, with a g value of 2.0036 was used for g factor calculations. Measurements at 77 K were made with a quartz dewar, whose tail fitted into the JEOL multipurpose EPR cavity.

The second harmonic generation test on the crystals was performed by the Kurtz powder SHG method [25].

Results and discussion

FTIR spectral analysis

FTIR spectrum of Cu(II)-doped MRSH crystal is shown in Fig. 2. It shows a broadband at 3,400–3,000 cm^{-1}. This band is assigned for $\nu_{(OH)}$ of lattice and coordinated water molecules. A broadband appeared at 1,703–1,716 cm^{-1} indicates that it is due to the coordinated water molecules [26] in the Cu(II)-doped MRSH.

UV–VIS spectral studies

An absorption spectrum will show a number of absorption bands corresponding to structural groups within the molecule. Different molecules absorb radiation of different wavelengths. Absorbance is inversely proportional to transmittance. From the UV spectrum (Fig. 3) of Cu(II)-doped MRSH, it is evident that the absorbance is meager around λ_{abs} 1.537, and hence transmittance is maximum.

SEM and EDS studies

The investigation of the influence of the dopant Cu(II) on the surface morphology of MRSH crystal faces reveals the

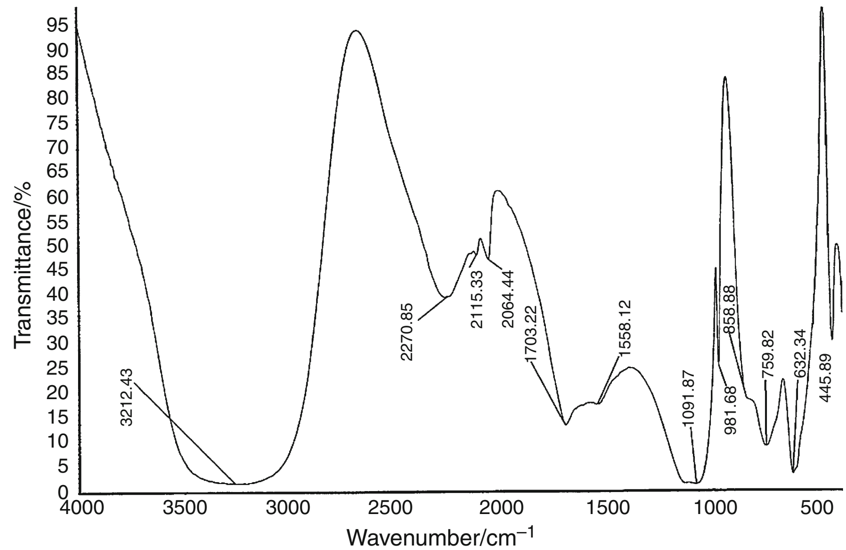

Fig. 2 FTIR spectrum of Cu(II)-doped MRSH

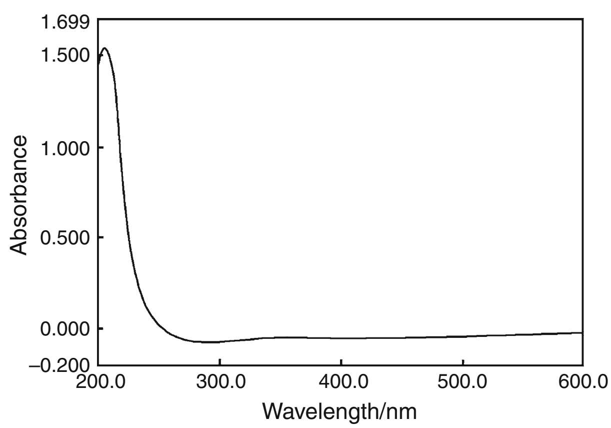

Fig. 3 UV spectrum of Cu(II)-doped RSH

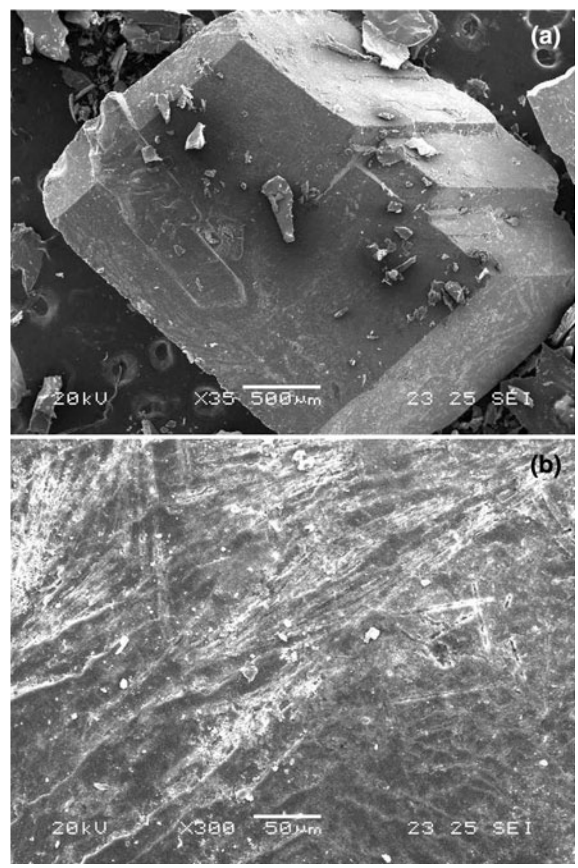

Fig. 4 SEM photographs of Cu(II)-doped MRSH **a** ×35 and **b** ×300 magnifications

formation of structure defect centers (Fig. 4a, b). At 300 magnifications, layered structure was observed. The presence of Cu^{2+} ions in the doped specimen was confirmed by EDS (Fig. 5). Bhagavannarayana et al. [24] have shown that ADP crystals grown in the presence of KCl contain K^{+} ions. The amount of Cu(II) incorporation into the MRSH lattice is shown in Table 1. From the table, it is evident that magnesium rubidium sulfate has formed a lattice in which the doped Cu(II) has entered the crystal lattice.

Thermal analysis

The thermodynamic data of Cu(II)-doped MRSH crystal was calculated from TG-DTA curves given in Fig. 6. The thermodynamical data are calculated using Coats–Redfern (CR) [27], Doyle' (Dy) [28], and Horowitz–Metzger (HM) [29] methods. The calculated thermodynamic values are summarized in the Tables 2 and 3. Copper-doped mixed salt are thermally stable up to 347 K where the decomposition starts and ends at 573 K accompanied with a sharp mass loss of about 21% with corresponding strong endothermic DTA peak at 491 K. The frequency value (A) calculated by all these methods [27–29] show a high value and also a positive entropy of activation, and it appears that the faster rate of dehydration of Cu(II)-doped MRSH complex.

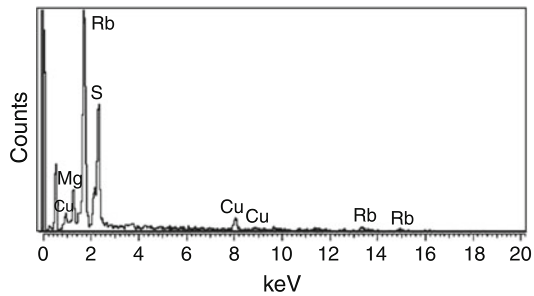

Fig. 5 EDS spectrum of Cu(II)-doped MRSH

Table 1 EDS data of Cu(II)-doped MRSH crystal

Elements	Weight/%	Atomic/%
Mg	5.56	11.92
S	27.88	45.31
Cu	10.38	8.51
Rb	56.19	34.26
Total	100.00	100.00

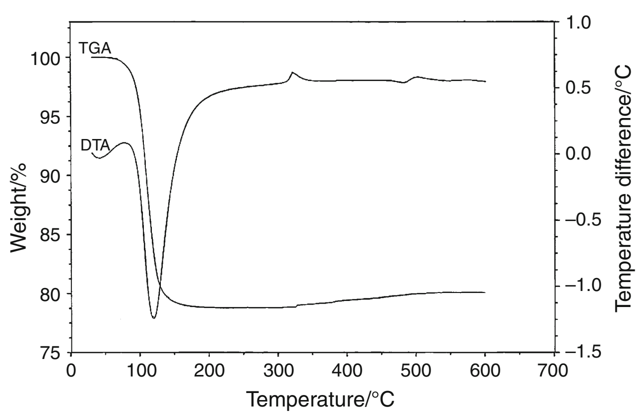

Fig. 6 TG-DTA curves of Cu(II)-doped MRSH

Table 2 Decomposition data of Cu(II)-doped MRSH

Temperature/K	$1/T$	θ	α	ln $(-\ln(1-\alpha)/T_2)$	ln $(-\ln(1-\alpha))$
361	0.002770	−30	0.061167	−14.5405	−2.76275
369	0.002710	−22	0.122334	−13.8581	−2.03646
371	0.002695	−20	0.183501	−13.4283	−1.59588
373	0.002681	−18	0.244668	−13.1140	−1.27083
375	0.002667	−16	0.306337	−12.8596	−1.00575
377	0.002653	−14	0.370512	−2.6348	−0.77035
379	0.002639	−12	0.428671	−12.4553	−0.58019
381	0.002625	−10	0.489838	−12.2816	−0.39597
383	0.002611	−8	0.551005	−12.1183	−0.22221
385	0.002597	−6	0.612173	−11.9607	−0.05425
387	0.002584	−4	0.673340	−11.8046	0.11229
389	0.002571	−2	0.734507	−11.6449	0.28229
391	0.002558	0	0.795674	−11.4749	0.46250
393	0.002545	2	0.856841	−11.2830	0.66465
395	0.002532	4	0.918008	−11.0410	0.91675

Table 3 Thermodynamic data of Cu(II)-doped MRSH

Method	ΔH/ kJ mol^{-1}	$-\Delta S$/J K^{-1} mol^{-1}	E_a/ kJ mol^{-1}	A/s^{-1}	R
Coats–Redfern	20.54	52.53	120.81	4.52E + 15	0.99
Doyle's	32.21	82.39	127.11	1.64E + 17	0.995
Horowitz–Metzger	40.53	103.66	134.73	2.11E + 18	0.993

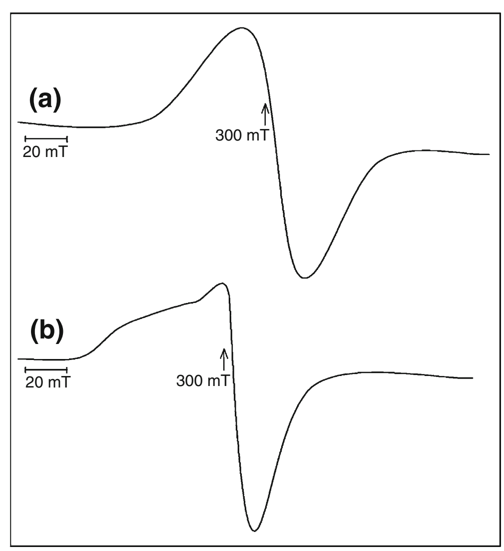

Fig. 7 Powder EPR spectra of (*a*) Cu(II)-doped MRSH at room temperature, $\nu = 9.39718$ GHz and (*b*) Cu(II)-doped MRSH at 77 K, $\nu = 9.07971$ GHz

EPR spectral analysis

Powder EPR spectrum of Cu(II)-doped MRSH is given in Fig. 7a, which was recorded at room temperature. It shows axially symmetric nature and the calculated g values are $g_{\parallel} = 2.466$ and $g\perp = 2.204$. This spectrum does not show any hyperfine from copper nucleus. Figure 7b shows the EPR spectrum of Cu(II)-doped MRSH recorded at 77 K. A small shift in 'g' values is noticed as the temperature of the sample is reduced. This confirms that the paramagnetic impurity Cu(II) has entered the MRSH lattice interstitially. It has been reported [4] that doping of VO(II) impurity in the crystal lattice of magnesium potassium Tutton's salt results in both substitutional and interstitial occupancy.

Second harmonic generation efficiency

A Nd:YAG laser with a modulated radiation of wavelength 1,064 nm was used as the optical source and directed on the powder sample through a filter. The doubling of frequency was confirmed by the green radiation of wavelength 532 nm. This study reveals that the crystal MRSH has got SHG efficiency and no variation is found on doping of Cu(II) in MRSH.

Conclusions

The incorporation of Cu^{2+} in the crystalline matrix of MRSH crystal is confirmed by EDS spectra. SEM reveals the different morphology in the presence of the dopant. UV–VIS spectra of the doped sample clearly indicate the good transparency throughout the entire UV–VIS region. This property makes it suitable for the fabrication of optical device. FTIR spectrum confirms the presence of coordinated water molecule of the complex. TG-DTA studies reveal the faster rate of dehydration of Cu(II)-doped MRSH crystal. Powder EPR spectrum of the Cu(II)-doped MRSH recorded both in room temperature and at 77 K reveal the interstitial occupancy of the dopant. Doping has no effect on the NLO property.

References

1. Tutton AE. A comparative crystallographic study of the double selenites of the series $R_2M(SeO_4)_2{\cdot}6H_2O$-salts in which M is zinc. Proc R Soc Lond. 1900;67:58–84.
2. Anandalakshmi H, Rajendiran TM, Venkatesan R, Sambasiva Rao P. Single crystal EPR study of VO(II)-doped magnesium potassium Tutton's salt—Part 4. Spectrochim Acta A. 2000;56: 2617–25.
3. Sambasiva Rao P. Single-crystal EPR study of Fe(III)-doped magnesium potassium Tutton's salt—Part 3. Spectrochim Acta A. 1996;52:1127–34.
4. Sambasiva Rao P. Single crystal EPR study of Mn(II)-doped magnesium potassium Tutton's salt. Spectrochim Acta A. 1993;49:897–901.
5. Bleaney B, Penrose RP, Plumpton BI. Paramagnetic resonance in the copper Tutton salts. Proc R Soc Lond A. 1949;198:406–28.
6. Sastry B, Sastry GS. Electron spin resonance studies on Cu^{2+} doped $Na_2Zn(SO_4)_2{\cdot}4H_2O$. J Phys C. 1971;4:L347.
7. Keeiah RM, Rao JL, Chand P, Lakshman SVJ. Electron paramagnetic resonance study of copper(II) ions in single crystal of thallium magnesium sulfate hexahydrate. Phys Status Solidi B. 1989;151:615–21.
8. Silver BL, Getz DJ. ESR of $Cu^{2+}(H_2O)_6$. II. A quantitative study of the dynamic John Teller effect in copper doped zinc Tutton's salt. J Chem Phys. 1974;61:638–50.
9. Fuji Y, Shigi T. Thermal and magnetic properties of copper potassium Tutton salt below 0.15 K. J Low Temp Phys. 1988;72:267–82.
10. Manomenova VL, Rudneva EB, Malakhova LF, Furmanova NG, Voloshin AE, Smirnova TN. Crystal growth and properties of $Rb_2Ni(SO_4)_2{\cdot}6H_2O$ (RNSH). Crystallogr Rep. 2007;52:918–22.
11. Ravi S, Subramanium P. Electron paramagnetic resonance and optical studies of Cu^{2+} doped bis(thiourea)cadmium chloride single crystal. Solid State Sci. 2007;9:961–3.
12. Meenakshisundram S, Parthiban S, Bhagavannarayana G, Madhurambal G, Mojumdar SC. Influence of organic solvent on tristhioureazinc(II)sulphate crystals. J Therm Anal Calorim. 2009;96:125–9.
13. Swiderski G, Kalinowska M, Wojtulewski S, Lewandowski W. Experimental (FT-IR, FT-Raman, ^{1}H NMR) and theoretical study of magnesium, calcium, strontium and barium picolinates. Spectrochim Acta A. 2006;64:24–33.
14. Flakus HT, Jablonska M. Study of hydrogen bond polarized IR spectra of cinnamic acid crystals. J Mol Struct. 2004;707:97–108.
15. Hanai K, Kuwae A, Takai T, Senda H, Kunimoto K. A comparative vibrational and NMR study of *cis*-cinnamic acid polymorphs and *trans*-cinnamic acid. Spectrochim Acta A. 2001;57:513–9.
16. Hsich T, Su C, Su C, Chen C, Liou CH, Li-Hwa L. Using experimental studies and theoretical calculations to analyze the molecular mechanism of coumarin, *p*-hydroxybenzoic acid and cinnamic acid. J Mol Struct. 2005;741:193–9.
17. Vasudevan G, Anbusrinivasan P, Madhurambal G, Mojumdar SC. Thermal analysis, effect of dopants, spectral characterization and growth aspects of KAP crystals. J Therm Anal Calorim. 2009;96:99–102.
18. Meenakshisundaram S, Parthiban S, Pisipaty UR, Madhurambal G, Mojumdar SC. Effect of anthracene doping on potassium hydrogen phthalate crystals. J Therm Anal Calorim. 2010;100:821–6.
19. Kalinowska M, Siemieniuk E, Kostro A, Lewandowski W. The application of Aj, BAC, I6, HOMA indexes for quantitative determination of aromaticity of metal complexes with benzoic, salicylic, nicotinic acids and benzene derivatives. J Mol Struct. 2006;761:129–41.
20. Anbusrinivasan P, Madhurambal G, Mojumdar SC. *p*-*N*,*N*-dimethylaminobenzaldehyde (DAB) grown by solution technique using CCl4 as growth medium. J Therm Anal Calorim. 2009;96:111–5.
21. Muthu K, Bhagavannarayana G, Chandrasekaran C, Parthiban S, Meenakshisundaram SP, Mojumdar SC. Os(VIII) doping effects on the properties and crystalline perfection of potassium hydrogen phthalate (KHP) crystals. J Therm Anal Calorim. 2010;100:793–9.
22. Parthiban S, Murali S, Madhurambal G, Meenakshisundaram SP, Mojumdar SC. Effect of zinc(II) doping on thermal and optical properties of potassium hydrogen phthalate (KHP) crystals. J Therm Anal Calorim. 2010;100:751–6.
23. Kasthuri L, Bhagavannarayana G, Parthiban S, Ramasamy G, Muthu K, Meenakshisundaram SP. Rare earth cerium doping effects in nonlinear optical materials: potassium hydrogen phthalate (KHP) and tris(thiourea)zinc(II) sulfate (ZTS). CrystEngComm. 2010;12:493–9.
24. Bhagavannarayana G, Parthiban S, Meenakshisundaram S. An interesting correlation between crystalline perfection and second harmonic generation efficiency on KCl- and oxalic acid-doped ADP crystals. Cryst Growth Des. 2008;8:446–51.
25. Kurtz SK, Perry TT. A powder technique for the evaluation of nonlinear optical materials. J Appl Phys. 1968;39:3798–813.
26. Nakamoto K. Raman Infrared spectra of inorganic, coordination compounds. 4th ed. New York: Wiley; 1986. p. 242–4.
27. Coats AW, Redfern JP. Kinetic parameters from thermogravimetric data. Nature. 1964;201:68–9.
28. Doyle CD. Kinetic analysis of thermogravimetric data. J Appl Polym Sci. 1961;5:285–92.
29. Horowitz HH, Metzger G. A new analysis of thermogravimetric traces. Anal Chem. 1963;35:1464–8.